AD-A148 532   OPTIMUM PERFORMANCE PARAMETERS FOR SKI-JUMP OPERATIONS   1/1
OF USAF FIGHTER AIRCRAFT(U) AIR FORCE WRIGHT
AERONAUTICAL LABS WRIGHT-PATTERSON AFB OH J J OLSEN
UNCLASSIFIED   AUG 84 AFWAL-TM-84-217-FIB   F/G 1/2   NL

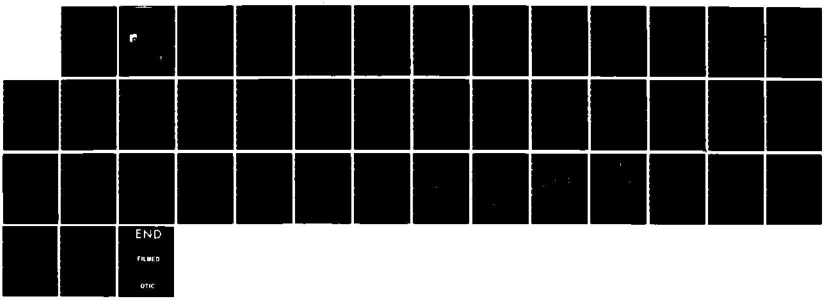

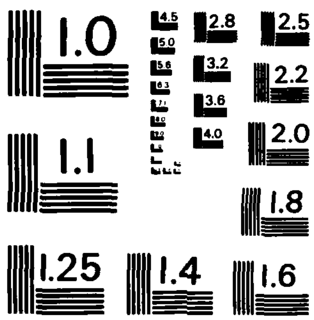
1.0
1.1
1.25
1.4
1.6
1.8
2.0
2.2
2.5
2.8
3.2
3.6
4.0
4.5
5.0
5.6

AFWAL-TM-84-217-FIB

OPTIMUM PERFORMANCE PARAMETERS FOR SKI-JUMP OPERATIONS OF USAF FIGHTER AIRCRAFT

JAMES J. OLSEN

AUGUST 1984

STRUCTURES & DYNAMICS DIVISION
FLIGHT DYNAMICS LABORATORY
AIR FORCE WRIGHT AERONAUTICAL LABORATORIES
WRIGHT-PATTERSON AIR FORCE BASE, OHIO 45433

FOREWORD

This report was prepared by Dr James J. Olsen of the Structures and Dynamics Division, Flight Dynamics Laboratory, Wright-Patterson Air Force Base, Ohio. The work was performed under Project 2401, "Aerospace Structures and Dynamics."

The ultimate purpose of the work is to define the aircraft structural loads and operational limitations involved in ski-jump operations of USAF fighter aircraft. This initial study concentrated on the aerodynamic performance aspects of the problem, to provide the speeds, weights, and geometric parameters needed for subsequent assessment of the structural aspects.

OPTIMUM PERFORMANCE PARAMETERS FOR SKI-JUMP OPERATIONS OF USAF FIGHTER AIRCRAFT

Abstract

This paper discusses the equations of motion which govern the aerodynamic performance of USAF fighter aircraft immediately after ski-jump takeoffs. By a careful selection of coordinate systems and independent and dependent variables, we eliminate the need for repetitive time-history integration of the nonlinear, coupled equations. This allows a relatively simple, but exact solution of the problem. Detailed results are presented for the F-4, A-10, F-15 and F-16 for two cases --

- a nominal baseline of constant pitch attitude
- a "best possible" case which produces the lowest achieveable takeoff speeds.

TABLE OF CONTENTS

LIST OF FIGURES

LIST OF FIGURES (CONT'D)

SECTION 1. INTRODUCTION

There has been a great deal of recent interest within the United States Air Force in the potential of ski-jump operations for fighter aircraft. The British Royal Air Force employs ski-jumps for the AV-8, and the United States Navy has demonstrated ski-jump operations for the T-2, F-14 and F-18.

The concept of operations is simply that the aircraft is given a vertical component of velocity at a speed substantially less than flying speed. The angle of the ski-jump and the launch speed are established so that the aircraft accelerates to flying speed at a trimmed condition by the time it loses its vertical velocity component. The aircraft can be flown with controls fixed for some preselected condition, or the pilot can execute some control. However, the time interval is short (only a few seconds) during the trajectory, so the pilot's procedures must be simple and instinctive.

If the launch speed is too high, then the aircraft has used more runway distance than necessary and may experience higher structural loads on the ski-jump. If the launch speed is too low, then the aircraft will not be able to sustain a positive rate of climb. For a given ski-jump, the optimum launch speed probably is the one that just produces an inflection at a trimmed condition at minimum flying speed. (See Sketch)

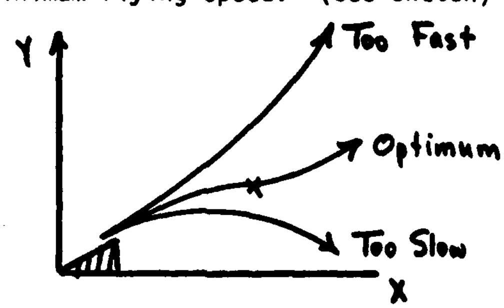

Generally, larger ramp angles also provide the desirable smaller launch speeds. However, there is a complicated interplay that must be considered among logistics, launch speed, ski-jump angle and aircraft loads. Also one must consider the sensitivity of the results to small errors in thrust and speed to provide adequate margins of safety.

The equations of motion which govern ski-jump performance are nonlinear and coupled, but fairly simple. Recent attacks on those equations have employed repetitive time-integrations over a host of values for the physical variables. This paper re-examines those equations of motion and shows that complete, exact solutions are easily obtained in the domain of airspeed, angle of attack and climb angle. There is no need for numerical integrations in time or distance. The process also shows the effects of the dominant nondimensional parameters and eliminates the need for large numbers of variations in the aircraft parameters for computed trajectories.

Section 2 derives the equations of motion; Section 3 gives numerical results for simplified aerodynamic representations of the F-4, A-10, F-15 and F-16 for two cases ((1) baseline and (2) optimum selections for angle of attack histories). Section 4 contains concluding remarks.

SECTION 2. METHOD OF ANALYSIS

2.1 EQUATIONS OF MOTION

The aircraft is assumed to be a rigid point mass with freedom to translate in the x and y directions and rotate in pitch.

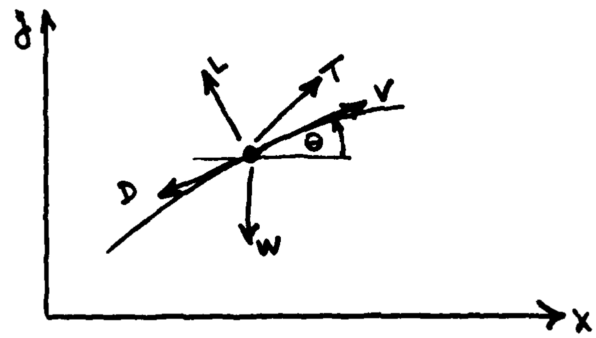

The forces acting are the Thrust (T), Lift (L), Drag (D) and Weight (W). The thrust is at an angle α_e above the fuselage reference line ; the fuselage reference line is at an angle α above the velocity vector (V); and the velocity is at an angle θ above the horizontal x axis. The pitch attitude (ψ) is given by

$$\psi = \alpha + \theta \tag{2.1}$$

The equations of motion for the three degrees of freedom in rectangular coordinates are

$$m\ddot{x} = T\cos(\alpha+\alpha_e+\theta) - D\cos\theta - L\sin\theta \tag{2.2}$$

$$m\ddot{y} = T\sin(\alpha+\alpha_e+\theta) + L\cos\theta - D\sin\theta - W \tag{2.3}$$

$$I\ddot{\psi} = M \tag{2.4}$$

where M is the pitching moment, and I is the moment of inertia about the center of mass. Together with the relation

$$\frac{dy}{dx} = \tan \Theta \qquad (2.5)$$

equations (2.1) through (2.4) are sufficient to solve for x, y, α, Θ, ψ as functions of time by integrating numerically in time from a set of initial conditions. Indeed many of the investigations of ski-jump performance have used such a straightforward technique. However, a problem with the numerical integration (in time) of the equations is the tedious nature of the process and the difficulty with gaining engineering insight into the effects of the many variables from the repeated, trial-and-error solutions.

2.2 A BETTER COORDINATE SYSTEM

A better approach is to abandon the fixed rectangular coordinates (x,y) and write the equations in the normal/tangential coordinates (n,s).

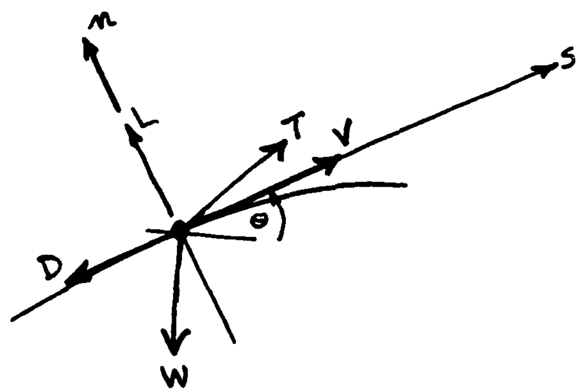

The equations of motion simplify to

$$m\ddot{s} = T\cos(\alpha+\alpha_e) - D - W\sin\theta \qquad (2.6)$$

$$m\ddot{n} = T\sin(\alpha+\alpha_e) + L - W\cos\theta \qquad (2.7)$$

$$I\ddot{\psi} = M \qquad (2.8)$$

The real advantage, however, comes when we replace time as the independent variable with tangential distance (s) by observing

$$\dot{s} = V \qquad (2.9)$$

$$\ddot{s} = V\frac{dV}{ds} \qquad (2.10)$$

$$\ddot{n} = V^2\frac{d\theta}{ds} \qquad (2.11)$$

$$\dot{\psi} = V\frac{d\psi}{ds} \qquad (2.12)$$

$$\ddot{\psi} = V^2\frac{d^2\psi}{ds^2} + V\frac{dV}{ds}\frac{d\psi}{ds} \qquad (2.13)$$

The equations of motion become:

$$mV\frac{dV}{ds} = T\cos(\alpha+\alpha_e) - D - W\sin\theta \qquad (2.14)$$

$$mV^2\frac{d\theta}{ds} = T\sin(\alpha+\alpha_e) + L - W\cos\theta \qquad (2.15)$$

$$I\left(V^2\frac{d^2\psi}{ds^2} + V\frac{dV}{ds}\frac{d\psi}{ds}\right) = M \qquad (2.16)$$

Now introduce the notation

$$\left.\begin{aligned} L &= C_L\frac{\rho V^2 A}{2} = C_L Q W \\ D &= C_D Q W \\ M &= C_M Q W c \\ Q &= \frac{\rho V^2 A}{2W} = \frac{q A}{W} \\ I &= m r^2 c^2 \\ \tau &= T/W \end{aligned}\right\} \qquad (2.17)$$

$$\varepsilon = \frac{\rho A c g}{W}$$

Then the exact equations of notion reduce to:

$$\frac{dQ}{ds} = \frac{\epsilon}{c}\left[\tau\cos(\alpha+\alpha_e) - C_D Q - \sin\Theta\right] = \frac{\epsilon}{c}\ddot{s}_g \qquad (2.18)$$

$$2Q\frac{d\Theta}{ds} = \frac{\epsilon}{c}\left[\tau\sin(\alpha+\alpha_e) + C_L Q - \cos\Theta\right] = \frac{\epsilon}{c}\ddot{n}_g \qquad (2.19)$$

$$2Q\frac{d^2\psi}{ds^2} + \frac{dQ}{ds}\frac{d\psi}{ds} = \frac{\epsilon}{r^2c^2}C_M Q \qquad (2.20)$$

Equations 2.1, 2.5, 2.18, 2.19 and 2.20 are sufficient to integrate numerically in distance s to solve for Q, α, Θ, and ψ. Time does not enter the problem.

Also note that the main dependent variable has been reduced to nondimensional variable

$$Q = \frac{qA}{W} = \rho\frac{V^2A}{2W} \quad ,$$

that the thrust effects are all contained in the ratio of thrust to weight

$$\tau = T/W$$

and that the angle of attack effects are all contained in the nondimensional parameters C_L, C_D and C_M.

2.3 ELIMINATION OF DISTANCE AS A VARIABLE

An even greater simplification occurs, however, if we divide equation (2.19) by (2.18) to obtain

$$2Q\left(\frac{d\Theta}{dQ}\right) = \frac{\tau\sin(\alpha+\alpha_e) + C_L Q - \cos\Theta}{\tau\cos(\alpha+\alpha_e) - C_D Q - \sin\Theta} \qquad (2.21)$$

We have eliminated the distance s from the solution and have found that:

- if we can somehow specify $\alpha = \alpha(\Theta, Q)$

  [Equivalent to Solving the Moment Equation]

- we can integrate equation (2.21) numerically in Q for a full solution of the problem.

There is no need for integrations in time or distance. The entire problem can be solved exactly in the Q, Θ, α domain; and the dominant nondimensional parameters of $\tau = T/W$, $C_L C_D$ are most apparent. For instance, if we solve equation (2.21) for $\Theta(Q,\alpha)$ for several values of $\tau = T/W$, all of the variations of temperature and density due to "hot day" or "cold day" will be automatically accounted for and contained in one set of curves from one computer run.

Observe also that the expression

$$\tau \sin(\alpha+\alpha_e) + C_L Q - \cos\Theta = \ddot{n}_g \qquad (2.22)$$

is just the acceleration normal to the flight path (in g's), and the expression

$$\tau \cos(\alpha+\alpha_e) - C_D Q - \sin\Theta = \ddot{s}_g \qquad (2.23)$$

is just the acceleration along the flight path (in g's).

2.4 HANDLING THE PITCHING MOMENT EQUATION

We revert to the original pitching moment equation

$$I\ddot{\psi} = M \qquad (2.4)$$

and note that we can write

$$\dot{\psi} = \frac{d\psi}{dQ}\frac{dQ}{dt} = \frac{d\psi}{dQ}\cdot\frac{dQ}{ds}\cdot\frac{ds}{dt}$$

$$= \frac{d\psi}{dQ}\cdot\frac{dQ}{ds}\cdot V$$

$$= \sqrt{\frac{2W}{\rho A}}\sqrt{Q}\cdot\frac{dQ}{ds}\cdot\frac{d\psi}{dQ} \qquad (2.24)$$

$$\ddot{\psi} = \left(\frac{2W}{\rho A}\right)\sqrt{Q}\cdot\frac{dQ}{ds}\cdot\frac{d}{dQ}\left[\sqrt{Q}\cdot\frac{dQ}{ds}\cdot\frac{d\psi}{dQ}\right] \qquad (2.25)$$

After some algebraic manipulation the pitching moment equation becomes

$$\frac{d}{dQ}\left[\sqrt{Q}\cdot\frac{dQ}{ds}\cdot\frac{d\psi}{dQ}\right] = \frac{\epsilon\sqrt{Q}\,C_M}{2r^2c^2\cdot\left(\frac{dQ}{ds}\right)} \qquad (2.26)$$

where $\frac{dQ}{ds}$ will come from the equation

$$\frac{dQ}{ds} = \frac{\varepsilon}{c}\left[\tau \cos(\alpha+\alpha_e) - C_D Q - \sin\Theta\right] . \qquad (2.18)$$

If we abbreviate:

$$\frac{dQ}{ds} = \frac{\varepsilon}{c} F \qquad (2.27)$$

then the moment equation becomes:

$$\frac{d}{dQ}\left\{\sqrt{Q}\cdot F\cdot \frac{d\psi}{dQ}\right\} = \frac{C_M \sqrt{Q}}{2\varepsilon r^2 F} \qquad (2.28)$$

$$\text{with } F = \tau \cos(\alpha+\alpha_e) - C_D Q - \sin\Theta = \ddot{s}_g \qquad (2.29)$$

The most complete solution process then is to integrate the moment equation (2.28) simultaneously with the combined lift/drag equation (2.21) with Q as the independent variable.

Again, there is no need for numerical integrations in time or distance!

2.5 SUMMARY OF TECHNIQUES

The exact solutions of the aerodynamic performance for ski-jump operations for a rigid airplane, considered as a point mass with weight and moment of inertia, are given by simultaneous numerical integrations of:

$$2Q\left(\frac{d\Theta}{dQ}\right) = \frac{\tau \sin(\alpha+\alpha_e) + C_L Q - \cos\Theta}{F} \qquad (2.21)$$

and

$$\frac{d}{dQ}\left[\sqrt{Q}\cdot F \cdot \frac{d\psi}{dQ}\right] = \frac{C_M \sqrt{Q}}{2\varepsilon r^2 F} \qquad (2.28)$$

where $Q = \frac{qA}{W} = \frac{\rho V^2 A}{2W}$

and $F = \tau\cos(\alpha+\alpha_e) - C_D Q - \sin\theta = \ddot{s}_g$

The aerodynamic ccoefficients C_L, C_D and C_M would need to be obained as functions of α from available tabulated values or as analytical expressions.

The simultaneous numerical integration of both sets of equations has not been performed for this paper, rather we have considered two simplified alternatives to solving the moment equation:

a. As a nominal baseline, assume the pilot has enough control authority to hold α and C_M to values such that $\psi = \alpha + \theta$ is constant (Constant pitch attitude θ).

b. As limiting case, assume that the pilot has enough control authority to hold α and C_M to the "best" achievable values. The "best" values will be defined as those values of α which drive $\frac{dQ}{d\theta}$ toward large negative values. The pilot leaves the ski-jump at

$$Q_1 = Q_{launch}$$
$$\theta_1 = \theta_{ramp}$$

and accelerates to a trimmed condition

$$Q_2 = Q_{trim}$$
$$\theta_2 = 0$$

We know θ will decrease from θ_{ramp} to zero, and Q will increase from Q_1 to Q_2. Since we know Q_2, and we want Q_1 to be as small as possible, the "best" α will be the one that gives maximum $|\Delta Q/\Delta\theta|$.

References 1 and 2 contain descriptions of four computer programs which treat the two cases above. In each case we actually start the integrations from the trimmed flight condition and integrate the equations backwards in Q to the ski-jump starting points.

Reference 1 contains the programs which solve equation (2.21) under the assumption

$$\psi = \alpha + \theta = \text{constant.}$$

Reference 2 contains the programs which solve equation (2.21) under the assumption

$$\alpha = \alpha_{optimum} \text{ for best } \frac{dQ}{d\theta} .$$

In each case one program solves the equation for a fixed θ_{ramp} and a range of values for T/W, and one program solves the equations for a fixed T/W and a range of values for θ_{ramp}.

In order to solve equation (2.21) we need C_L and C_D as functions of α. Those values depend on many variables for any particular aircraft and are frequently given graphically or in tabular form. For the purposes of illustration in this paper we used the simple expressions

$$C_L = C_{L_\alpha} (\alpha - \alpha_{0L}) \qquad (2.29)$$

$$C_D = C_{D_0} + KC_L^2 \qquad (2.30)$$

The approximate values used for the results in Section 3 are:

A/C	$C_{L\alpha}$	α_{0L}	C_{D_0}	K	α_e
F-4	0.058	-2.0^0	0.092	0.13	0^0
A-10	0.100	-1.5	0.098	0.13	-5
F-15	0.071	-2.53	0.064	0.13	0
F-16	0.077	-5.0	0.070	0.13	0

These values are subject to considerable variation from one aircraft configuration to another and cg position. While the following results should be used mainly to illustrate the method and are only broadly indicative of the capabilities of any particular aircraft, we do find that the most important parameter is the ratio of thrust-to-weight, while the aerodynamic effects are smaller.

SECTION 3. RESULTS

3.1 THE "NOMINAL" CASE OF CONSTANT PITCH ATTITUDE

3.1.1 The 15 Degree Ramp

For purposes of establishing a baseline we assume that the pilot has the capability to control the aircraft such that

$$\psi = \alpha + \theta = \text{constant} = 15^\circ$$

where α = angle of attack

θ = climb angle

ψ = attitude relative to the horizon

The aircraft then leaves the ramp at

$$Q_1 = Q_{launch}$$
$$\alpha_1 = 0^\circ$$
$$\theta_1 = 15^\circ$$

and accelerates to a point of equilibrium flight:

$$Q_2 = Q_{trim}$$
$$\alpha_2 = 15^\circ$$
$$\theta_2 = 0^\circ$$

Figures 1-4 illustrate the behavior of the climb angle versus airspeed for values of T/W from 0.4 to 2.0 for the F-4, A-10, F-15 and F-16. Since the ratio of thrust to weight is a variable for each case, the differences in the results are attributable to the low speed lift and drag characteristics for each aircraft. Of course, the full range of T/W is not available for each of the aircraft considered. Figure 5 shows the effect of T/W on the launch and trim speeds. Obviously T/W is the primary influence on the performance, with the aerodynamic effects being smaller.

3.1.2 Variable Ramps

Again we assume that the pilot has the capability to control the aircraft such that

$$\psi = \alpha + \theta = \text{constant.}$$

However, in this case we fix T/W at a nominal value for each aircraft:

A/C	Weight	Thrust	T/W
F-4	58,000 lb	30,000 lb	0.52
A-10	41,000 lb	14,000 lb	0.34
F-15	56,000 lb	40,000 lb	0.71
F-16	35,000 lb	20,000 lb	0.57

and vary the ramp angles from 6^o to 20^o. The aircraft then leaves the ramp at

$$Q_1 = Q_{launch}$$
$$\alpha_1 = 0^o$$
$$\theta_1 = \theta_{ramp}\ (6, 8, 10, \ldots 20^o)$$

and accelerates to a point of equilibrium flight

$$Q_2 = Q_{trim}$$
$$\alpha_2 = \theta_{ramp}\ (6, 8, 10, \ldots 20^o)$$
$$\theta_2 = 0^o$$

Figures 6-9 illustrate the behavior of the climb angle versus airspeed for values of $\theta_{ramp} = 6, 8 \ldots 20^o$ for the F-4, A-10, F-15 and F-16. Figure 10 shows the summary effect of the ramp angle on the launch and trim speeds for the four aircraft. Clearly the best performance (lowest launch speed) is achieved at the larger ramp angles.

3.1.3 A Closer Look at the F-15

While the effect of ramp angle on the climb angle constitutes the initial criterion for success, we also have to consider other aspects such as

- o acceleration along the flight path
- o acceleration normal to the flight path
- o "efficiency" ($dQ/d\theta$)

Figures 11-13 show the effects on those variables for T/W = 0.4, 0.6,...2.0 and for $\theta_{ramp} = 15^0$. Figure 11 gives the acceleration along the flight path (in g's) for the F-15 and shows that T/W = 0.4 is about the minimum value for which positive acceleration occurs. Figure 12 gives the acceleration normal to the flight path (in g's) as the F-15 leaves the ramp (nearly -1g) and accelerates to the equilibrium point (0 g's normal acceleration).

For a given ramp angle (θ_{ramp}) we know we must accelerate to an equilibrium condition of $\theta_{trim} = 0$. The airspeed at equilibrium (Q_{trim}) will be fixed by instantaneous values of T/W, C_L and C_D at that point. However, we want to fly the "best" history of angle of attack such that Q_{launch} is as small as possible. Therefore we want to obtain the maximum ΔQ as θ decreases from θ_{launch} to $\theta_{trim} = 0$. So $\frac{dQ}{d\theta}$ is a measure of efficiency, and we want $\frac{dQ}{d\theta}$ to be as large a negative number as possible. Alternatively, we want $\frac{d\theta}{dQ}$ to be a negative number as close to zero as possible. Figure 13 shows $\frac{d\theta}{dQ}$ versus airspeed for the 15^0 ramp for various values of T/W. We would like to drive the values of $\frac{d\theta}{dQ}$ into the upper left hand corner of Figure 13.

For a nominal value of T/W = 0.71, Figures 14-16 show the effect of ramp angle on the acceleration along the flight path, the acceleration normal to the flight path, and the "efficiency" of the assumption $\psi = \alpha + \theta = \theta_{ramp}$ = constant.

3.2 THE "OPTIMUM" ANGLE OF ATTACK PROFILE FOR THE F-15

3.2.1 Maximum Angle of Attack of 15°

Again we want to launch the aircraft at conditions

$$Q_1 = Q_{launch}$$
$$\alpha_1 = 0^{\circ}$$
$$\theta_1 = 15^{\circ}$$

and accelerate to a point of equilibrium flight

$$Q_2 = Q_{trim}$$
$$\alpha_2 = 15^{\circ}$$
$$\theta_2 = 0^{\circ}$$

However, we do not require the angle of attack to be scheduled to obtain a constant pitch attitude. Rather, we allow the angle of attack to seek the values which drive $\frac{d\theta}{dQ}$ to negative values, as close to zero as possible. There must be a constraint, however, that

$$\alpha \leq \alpha_{max}$$

As an example, Figure 17 presents the climb angle vs airspeed for the F-15 with T/W = 0.71 and $\alpha \leq \alpha_{max} = 15°$. The trim point is defined as the value of Q which produces $\alpha = \alpha_{max}$, $\theta = 0$ and $\frac{d\theta}{dQ} = 0$. The points A, B, C, D are chosen by:

Point	Q	θ
Trim	0.66	0°
A	0.5	0.8°
B	0.4	3.1°
C	0.3	7.9°
D	0.2	18.1°

We actually start at the trim point and integrate the equations numerically with Q as the independent variable, θ as the main dependent variable, and α as a free parameter. Figure 18 illustrates the process.

At the trim point Q = 0.66 we already have $\theta = \frac{d\theta}{dQ} = 0.0$. We step back in Q to Q = 0.5 and search iteratively for values of θ and α which produce values of $\frac{d\theta}{dQ} = 0^-$ (Curve A). We find from curve A that if we set $\alpha = 19.1^o$ we can set $\frac{d\theta}{dQ} = 0^-$. However, since α must be $\leq$ than α_{max} (15^o), we must pick $\alpha = 15^o$.

We then step back again in Q to Q = 0.4 and search iteratively for best values of θ and α. Again we find values of α which will set $\frac{d\theta}{dQ} = 0^-$, , but they are greater than α_{max}, so we must pick $\alpha = \alpha_{max}(15^o)$.

In this case, since we set initially $\alpha_{trim} = \alpha_{max}$, we find that the best (achievable) α is just α_{max} along the entire trajectory. If we had selected $\alpha_{trim} < \alpha_{max}$, then there would have been a short transition region as the "best" angle of attack moved from α_{trim} to α_{max}. (We treat this aspect further in Section 3.2.3.)

Figures 17 and 18 were examples to illustrate the method. Figures 19-23 give more extensive results for the F-15 with T/W varied as a parameter. In each case since we set $\alpha_{trim} = \alpha_{max} = 15^o$, the "best" angle-of-attack is α_{max} throughout the entire trajectory.

Figure 19 shows climb angle for the F-15 versus airspeed for values of T/W from 0.6 to 2.0. In particular note that at climb angles of $\theta = 15^{o}$ we have the following required airspeeds for the "optimum" α , compared with the required airspeeds for "constant ψ " from Figure 1.

T/W	Q_{launch} Best α	Constant ψ
0.6	0.320	0.31
0.8	0.230	0.30
1.0	0.164	0.23
1.2	0.116	0.17
1.4	0.078	0.13
1.6	0.051	0.098
1.8	0.031	0.072
2.0	0.017	0.053

Figure 20 shows the acceleration along the flight path versus airspeed. At $\theta = 15^{o}$ and "optimum α ", we have the following values of acceleration (in g's) which are slightly lower than those for "constant ψ " from Figure 11.

T/W	$\ddot{S}_g$ Best α	Constant ψ
0.6	0.23	0.33
0.8	0.45	0.53
1.0	0.66	0.73
1.2	0.87	0.93
1.4	1.00	1.13
1.6	1.29	1.33
1.8	1.50	1.53
2.0	1.68	1.73

Figure 21 shows the acceleration normal to the flight path versus airspeed. At $\theta = 15^0$ and "optimum α " we have the following values of acceleration (in g's) which are markedly

T/W	$\ddot{n}_g$ Best α	$\ddot{n}_g$ Constant ψ
0.6	-0.41	-0.91
0.8	-0.47	-0.93
1.0	-0.49	-0.94
1.2	-0.51	-0.95
1.4	-0.50	-0.95
1.6	-0.49	-0.96
1.8	-0.47	-0.96
2.0	-0.43	-0.96

better than those for "constant ψ " from Figure 12. Clearly the fact that the "optimum α " is allowed to be large at the launch condition allows the aircraft to generate more lift than the "constant ψ " condition of nearly zero lift at that point.

Figure 22 shows the "efficiency" $\frac{d\theta}{dQ}$ versus airspeed for the "optimum α ". At = 15^0 we have the following values which are superior to those for "constant ψ " from Figure 13 for T/W less than 1.

T/W	$\frac{d\theta}{dQ}$ Best α	Constant ψ
0.6	-2.6	-3.4
0.8	-2.3	-3.0
1.0	-2.3	-2.9
1.2	-2.5	-3.0
1.4	-3.0	-3.2
1.6	-4.0	-3.7
1.8	-5.1	-4.3
2.0	-6.2	-5.3

Figure 23 gives the "bottom line" for the comparison of the results for "*optimum* α" with those for "constant ψ". Figure 23 plots launch and trim speeds versus T/W for

(a) $\psi = \alpha + \theta = 15^o$ = constant

(b) $\psi = \alpha + \theta$ = variable, but $\alpha = \alpha_{optimum} \leq 15^o$.

3.2.2 Variable Maximum Angles of Attack

Section 3.2.1 covered the case where $\alpha = \alpha_{optimum} (\leq 15^o)$ for T/W = 0.6, 0.8,...2.0. In this Section we evaluate the effects of various values of α_{max} = 8, 10,...20^o for a constant T/W at the nominal value of 0.71.

In each case we establish a trimmed condition at $\alpha = \alpha_{max}$ and $\theta = \frac{d\theta}{dQ} = 0.0$. We again integrate the equations backwards in airspeed Q, searching iteratively for the "best" values of α and Θ which drive $\frac{d\Theta}{dQ}$ toward 0^-. Again, however, we have the constraint that $\alpha \leq \alpha_{max}$.

Figure 24 illustrates the climb angle versus airspeed. Shown for comparison later are the points where Θ has increased from the trim point to a value $\Theta = \alpha_{max}$. Figures 25, 26 and 27 give the acceleration along the flight path, the acceleration normal to the flight path, and the "efficiency". Figure 28 gives the key result, the launch speeds. The trim speed is given by the conditions $\alpha = \alpha_{max}, \Theta = \frac{d\Theta}{dQ} = 0$. The launch speed for the case $\psi = \Theta_{ramp}$ is given by $\alpha = 0, \Theta = \Theta_{ramp}$. The launch speed for the case $\alpha = \alpha_{optimum}$ is given by $\Theta = \Theta_{ramp}$ and α is free to assume the "best" value less than α_{max}.

3.2.3 $\alpha_{trim} \leq \alpha_{max}$

The last case we consider is the case where we attempt to provide a margin of safety by stipulating that the angle-of-attack at the trim condition (α_{trim}) will be less than the maximum angle of attack (α_{max}), thereby trimming at a slightly higher speed.

As an example we consider the five cases for the F-15 and T/W = 0.71 (See Figure 29).

$\alpha_{trim} = \alpha_{max} = 15^0$

(1) Select α such that $\psi = \alpha + \Theta = 15^0$ = constant

(2) Select $\alpha_{optimum}$ such that $\frac{d\Theta}{dQ}$ is an optimum

$\alpha_{trim} = \alpha_{max} = 20^o$

(3) Select α such that $\psi = \alpha + \theta = 20^o$ = constant

(4) Select $\alpha_{optimum}$ such that $\frac{d\theta}{dQ}$ is an optimum

$\alpha_{trim} = 15^o, \alpha_{max} = 20^o$

(5) Select $\alpha_{optimum}$ such that $\frac{d\theta}{dQ}$ is an optimum

Figures 29 and 30 illustrate thee behavior of α and θ with airspeed for the five cases.

(1) α starts at the trimmed value of 15^o at Q = 0.66 and decreases to 0^o at the launch speed of Q = 0.32.

(2) α starts at the trimmed value of 15^o and remains constant at speeds down to as low as Q = 0.20. θ increases from trimmed value of 0^o to values larger than 15^o, depending on how low we go for launch conditions.

(3) α starts at the trimmed value of 20^o at Q = 0.46 and decreases to 0^o at the launch speed of Q = 0.21 and $\theta = 20^o$.

(4) α starts at the trimmed value of 20^o and remains constant at speeds down to as low as Q = 0.15. θ increases from the trimmed value of 0^o to values larger than 20^o, depending on how low we go for launch conditions.

(5) α starts out at a trimmed value of 15^{o} at Q = 0.66. The aircraft then follows an "optimum" angle of attack profile to $\alpha = 20^{o}$ at Q = 0.46, which is actually just the previous trimmed condition for $\alpha = 20^{o}$. It then follows the optimum angle of attack for case (4).

Figures 31, 32 and 33 give the corresponding results for acceleration along the flight path, acceleration normal to the flight path and "efficiency". Figure 32 is the most revealing in that it shows how the "optimum " profile keeps the acceleration normal to the flight path to smaller negative values by providing a substantial angle of attack in the low speed launch region.

SECTION 4. CONCLUDING REMARKS

This paper shows that the performance equations for ski-jump operations reduce to equations where:

- Nondimension flight speed $Q = \frac{\rho V^2 A}{2W}$ is the main independent variable, and climb angle θ is the main dependent variable.

- The main free parameter which governs the operation is the angle of attack as a function of airspeed and climb angle, $\alpha(Q,\theta)$.

- The results depend only on the behavior of the nondimensional ratio of thrust-to-weight (T/W) and $C_L(\alpha)$ and $C_D(\alpha)$.

- Strictly speaking $\alpha(Q,\theta)$ should be obtained by solving the pitching moment equation. We considered two simplified approximations. In the baseline case α is selected to maintain constant pitch attitude. In the "optimum" case α is selected to drive $\frac{d\theta}{dQ} \rightarrow 0^-$, thus providing minimum possible launch speeds.

We presented results for the F-4, A-10, F-15 andd F-16. In particular, from the results of one computer run it is possible to consolidate all of the results into one plot of launch and trim speed vs T/W (Figures 5 or 23) or of launch and trim speed vs θ_{ramp} (Figures 10 or 28).

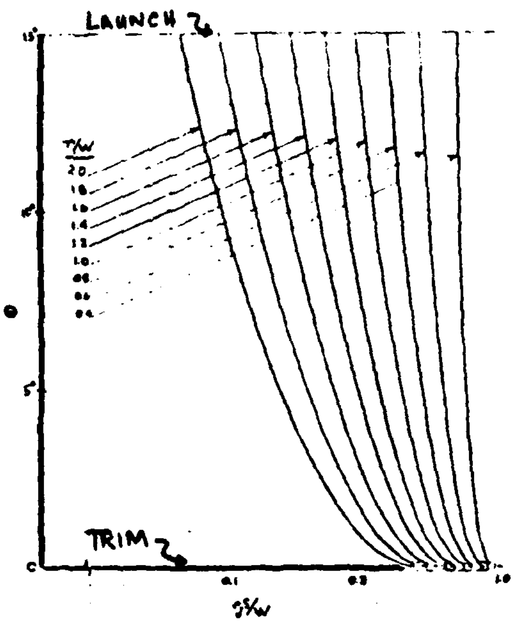

Figure 1. F-4

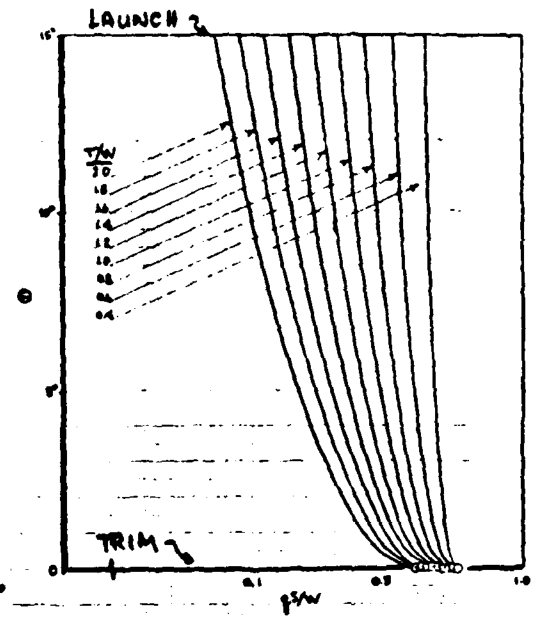

Figure 2. A-10

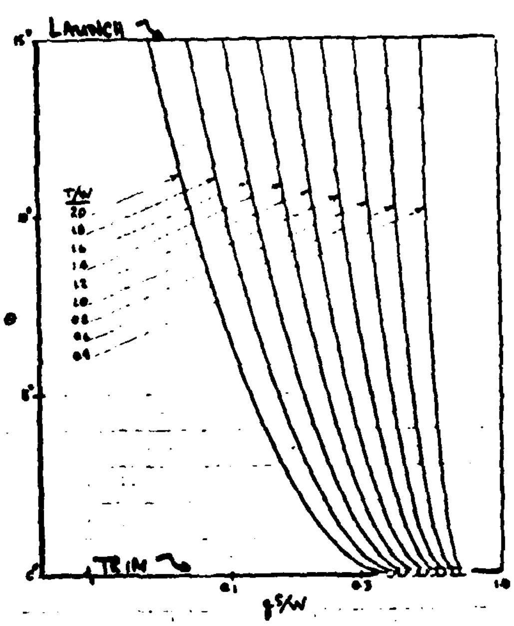

Figure 3. F-15

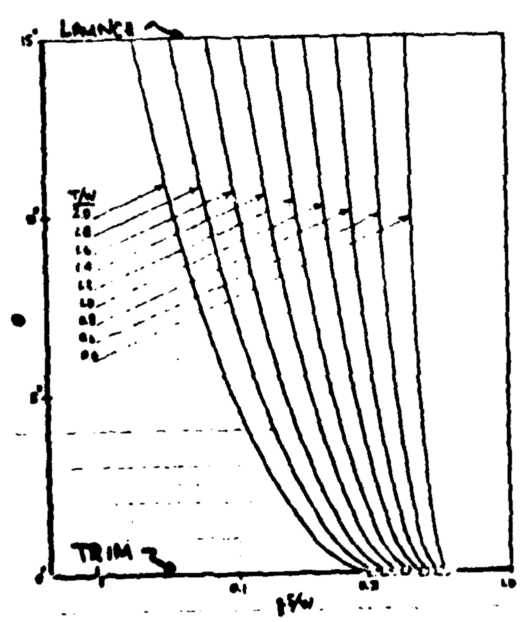

Figure 4. F-16

Climb Angles for a Constant Pitch Attitude ψ = 15°

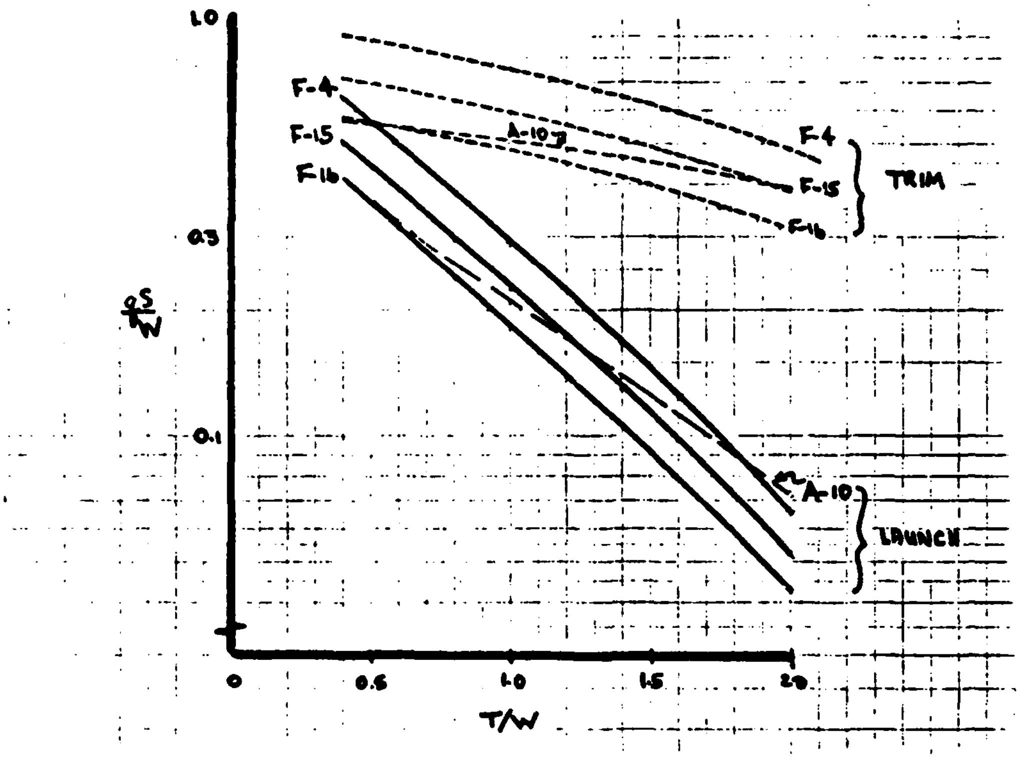

Figure 5. Launch and Trim Speeds for Constant Pitch Attitude ψ = 15°

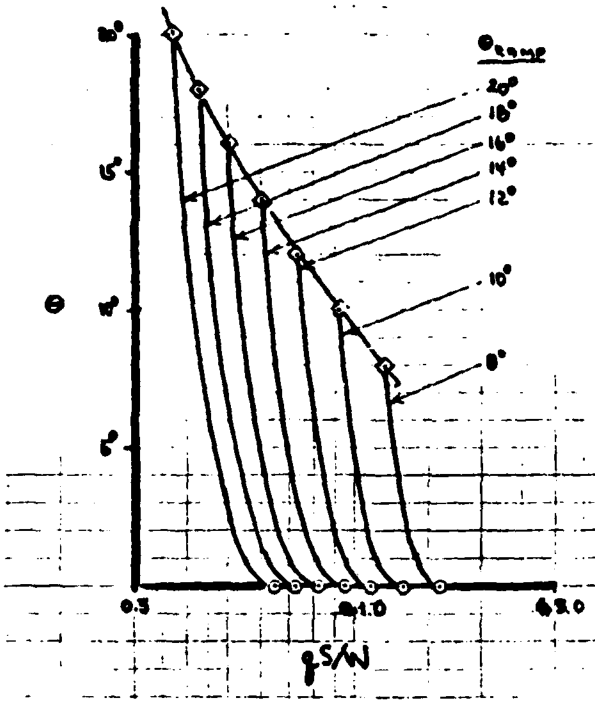

Figure 6. F-4, $\frac{T}{W}$ = 0.52

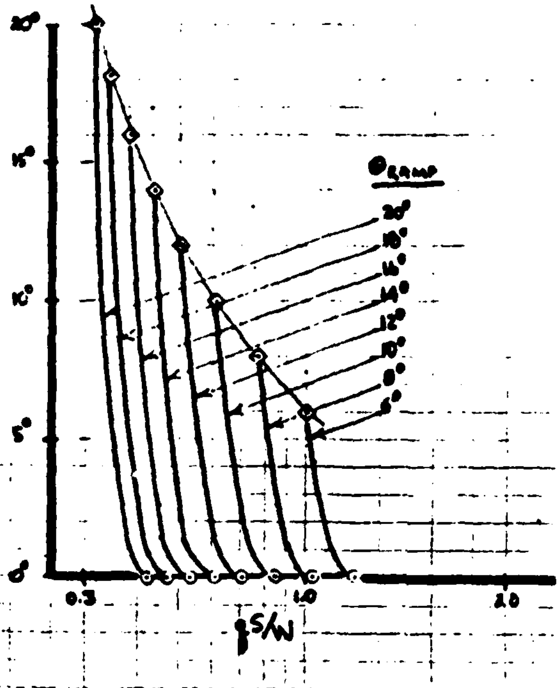

Figure 7. A-10, $\frac{T}{W}$ = 0.34

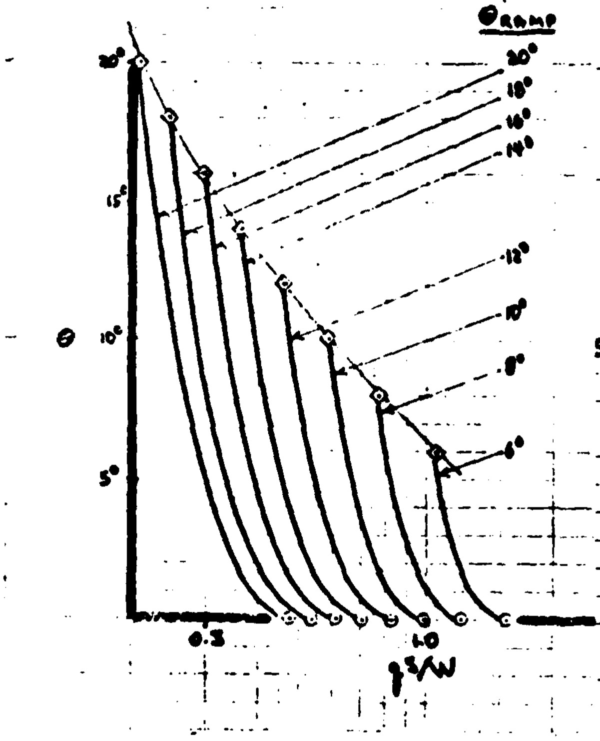

Figure 8. F-15, $\frac{T}{W}$ = 0.71

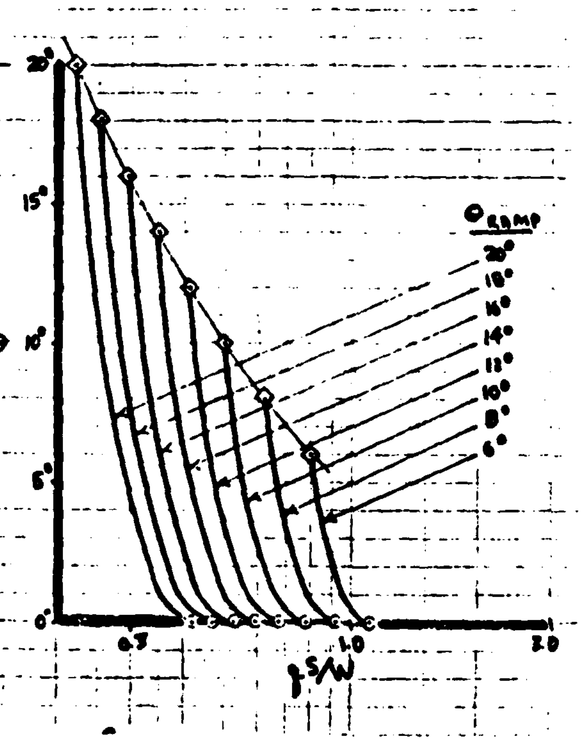

Figure 9. F-16, $\frac{T}{W}$ = 0.57

Climb Angles for Constant Pitch Attitude $\psi = \theta_{ramp}$ and Nominal T/W

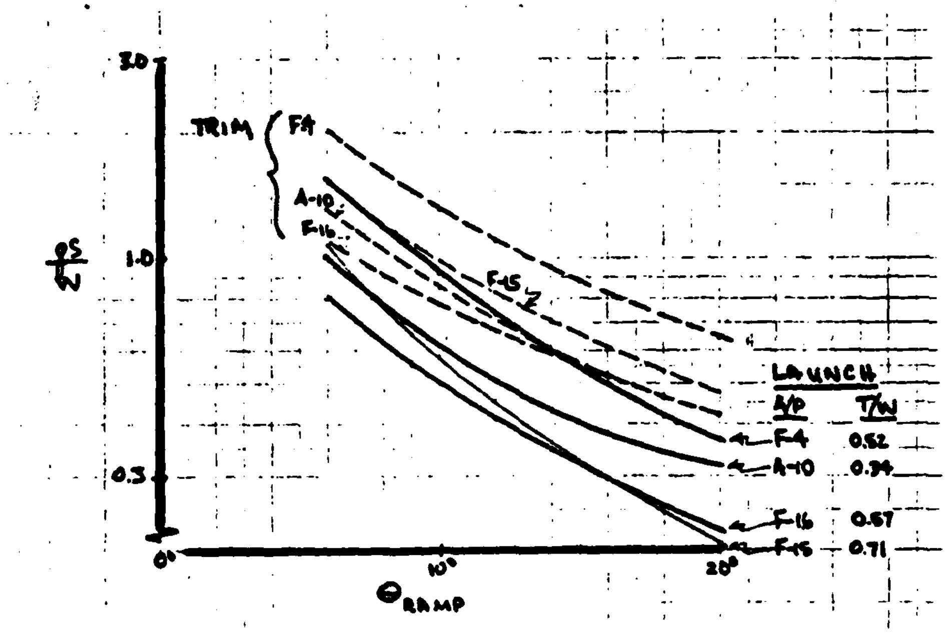

Figure 10. Launch and Trim Speeds for Constant Pitch Attitude $\psi = \theta_{ramp}$ and Nominal T/W

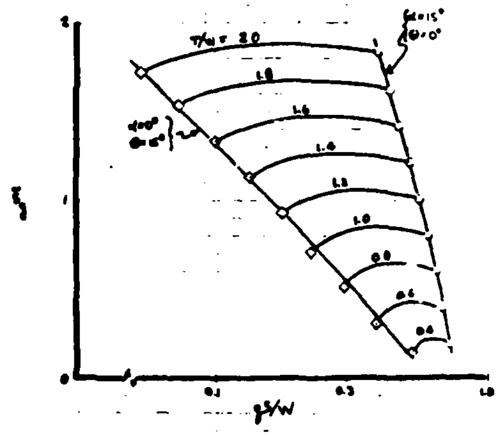

Figure 11. Acceleration Along the Flight Path

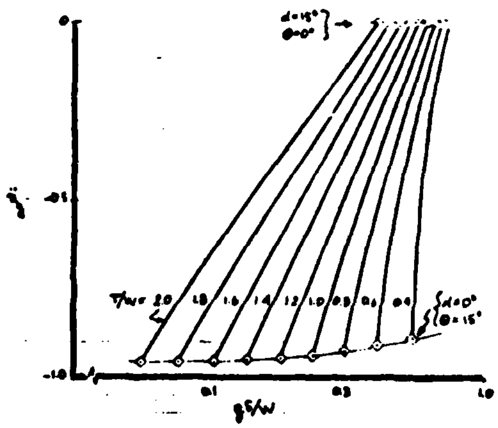

Figure 12. Acceleration Normal to the Flight Path

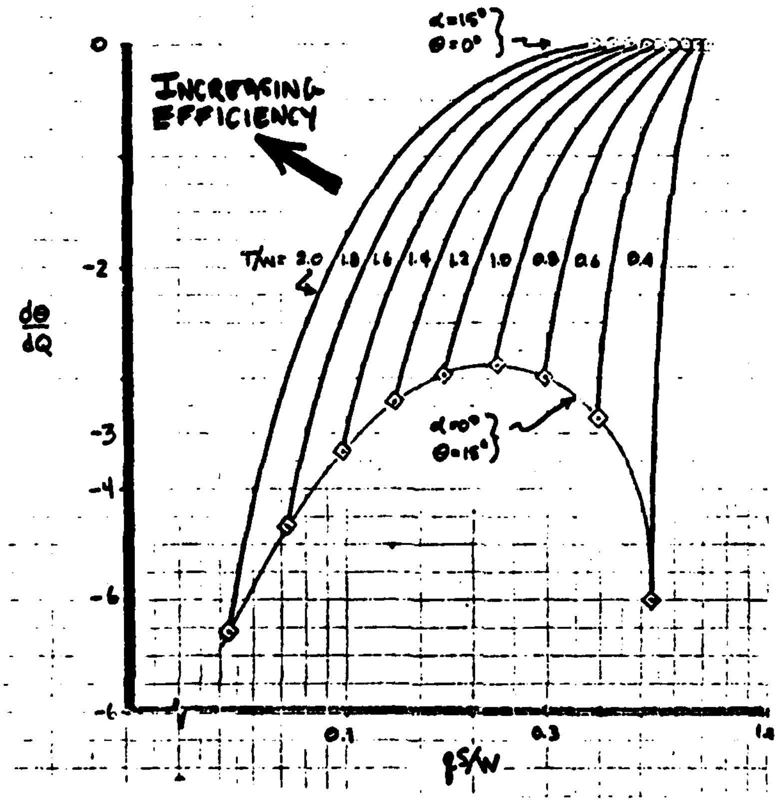

Figure 13. Efficiency

Performance of the F-15 at Constant Pitch Attitude $\psi = 15°$

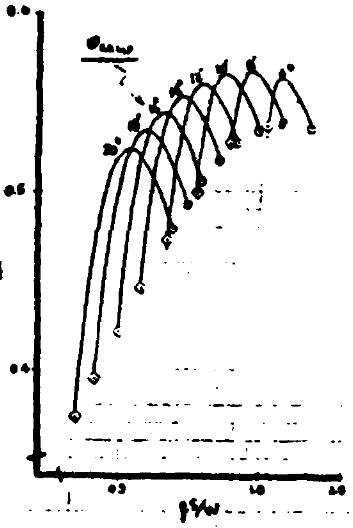

Figure 14. Acceleration Along the Flight Path

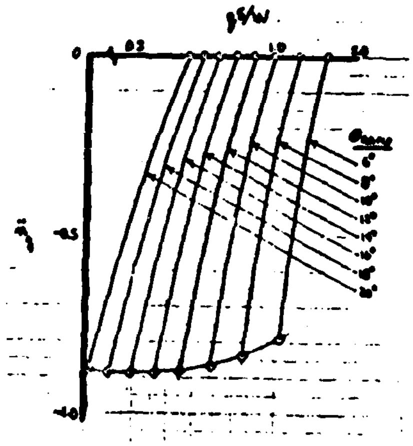

Figure 15. Acceleration Normal to the Flight Path

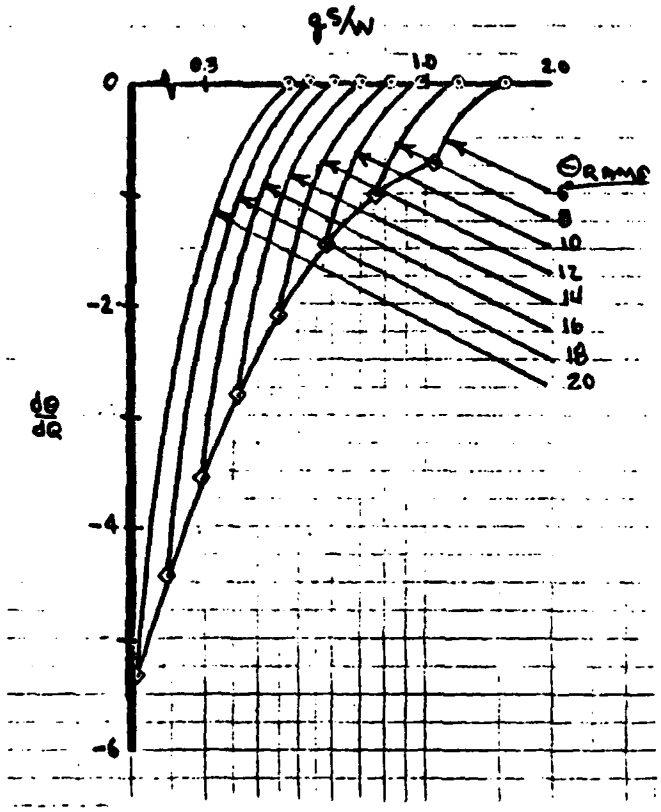

Figure 16. Efficiency

Performance of the F-15 at Constant Pitch Attitude $\psi = \theta_{ramp}$ and T/W = 0.71

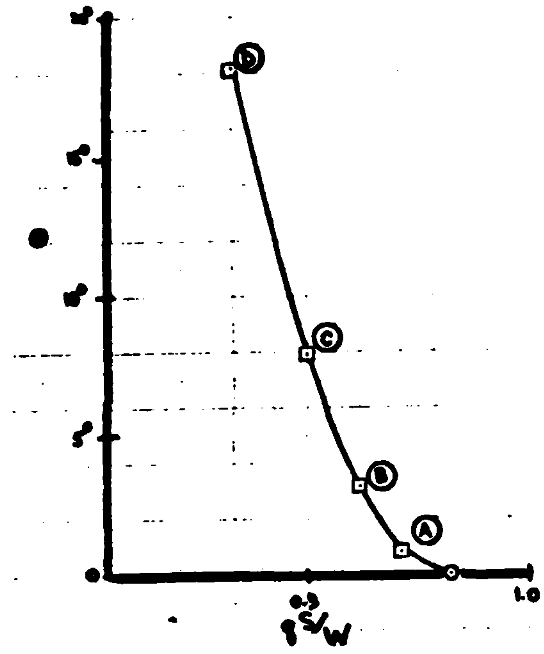

Figure 17. Climb Angle

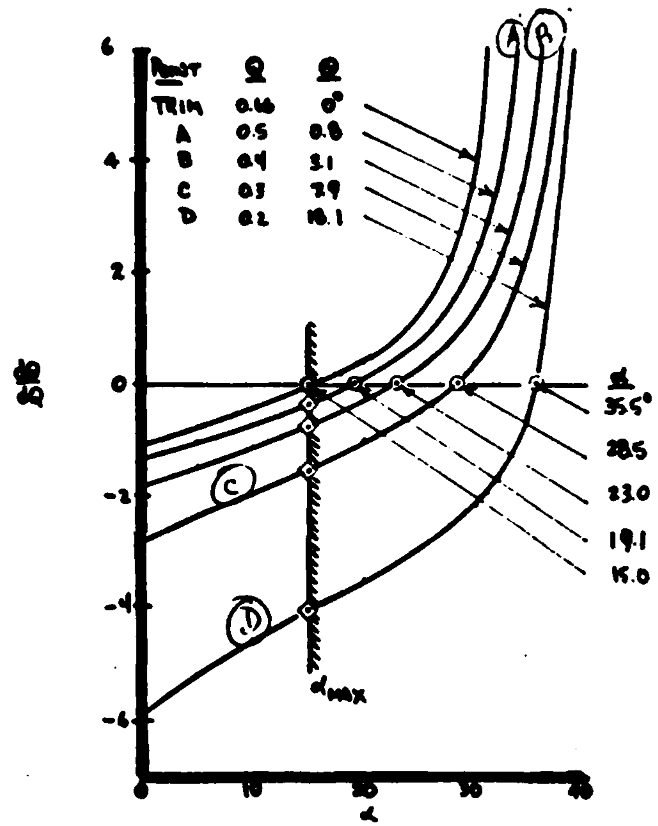

Figure 18. Efficiency

Selection of Angle of Attack for "Best" Efficiency for the F-15, $\alpha \leq 15°$, T/W = 0.71

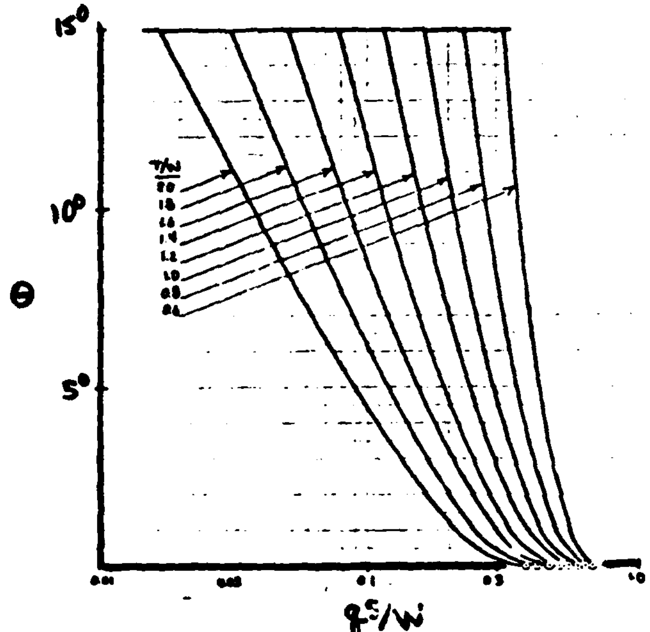

Figure 19. Climb Angle

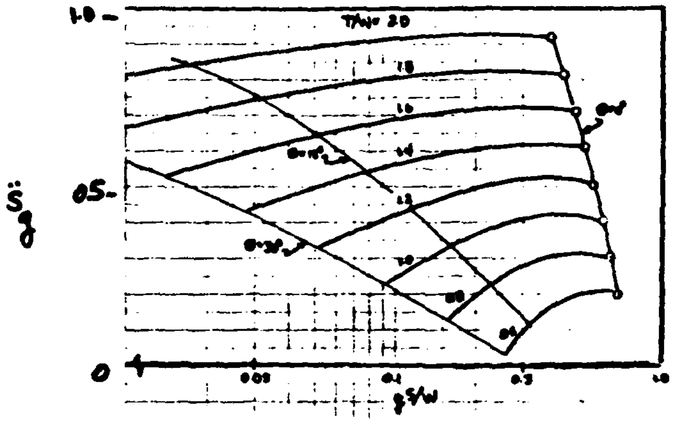

Figure 20. Acceleration Along the Flight Path

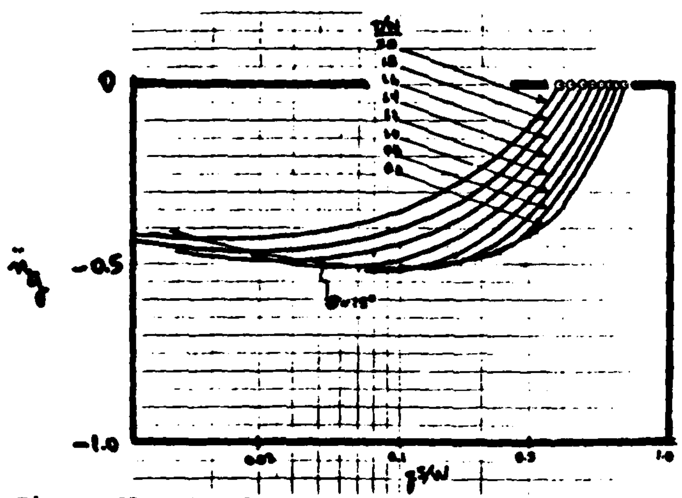

Figure 21. Acceleration Normal to the Flight Path

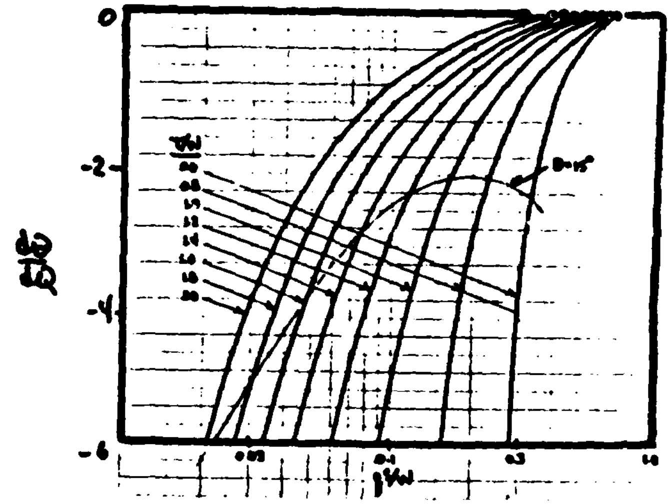

Figure 22. Efficiency

Performance of the F-15, $\alpha = \alpha_{optimum}$ ($\leq 15°$)

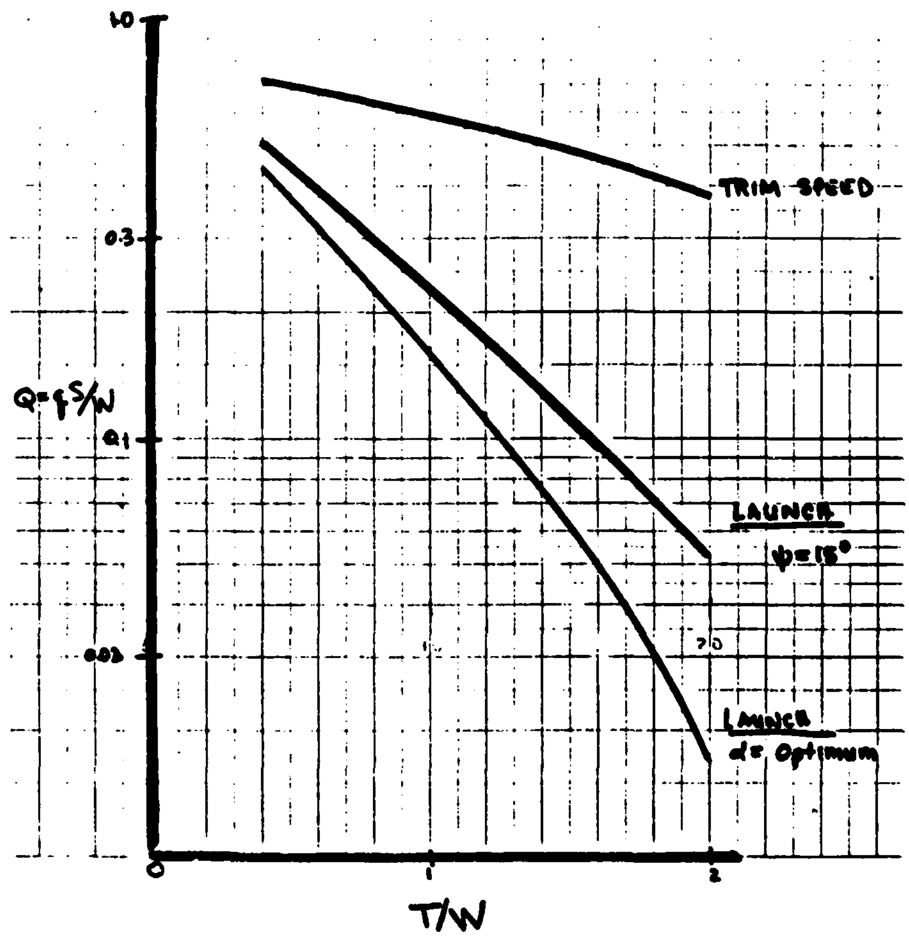

Figure 23. Launch and Trim Speeds for ψ = constant (15°) and for $\alpha = \alpha_{optimum}$ ($\leq$ 15°)

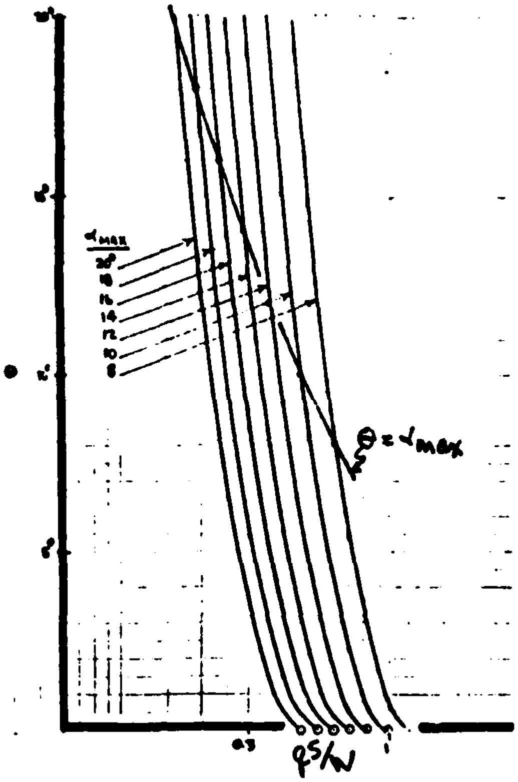

Figure 24. Climb Angle

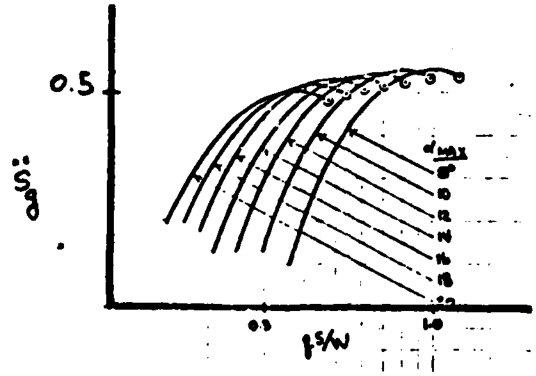

Figure 25. Acceleration Along the Flight Path

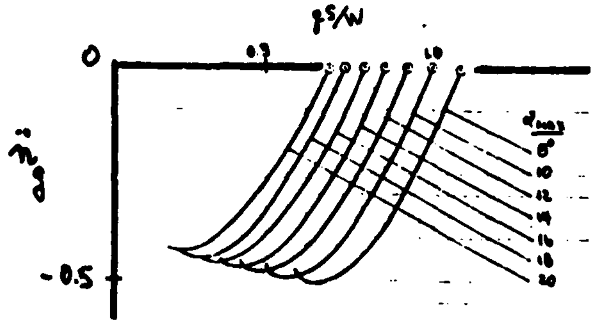

Figure 26. Acceleration Normal to the Flight Path

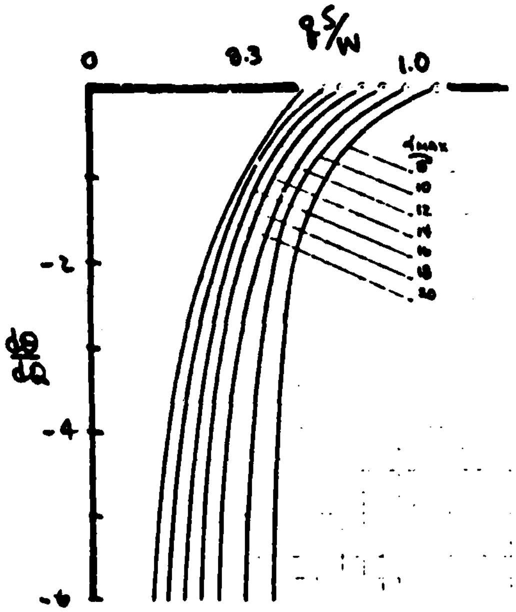

Figure 27. Efficiency

Performance of the F-15 for $\alpha = \alpha_{optimum}$ and T/W = 0.71

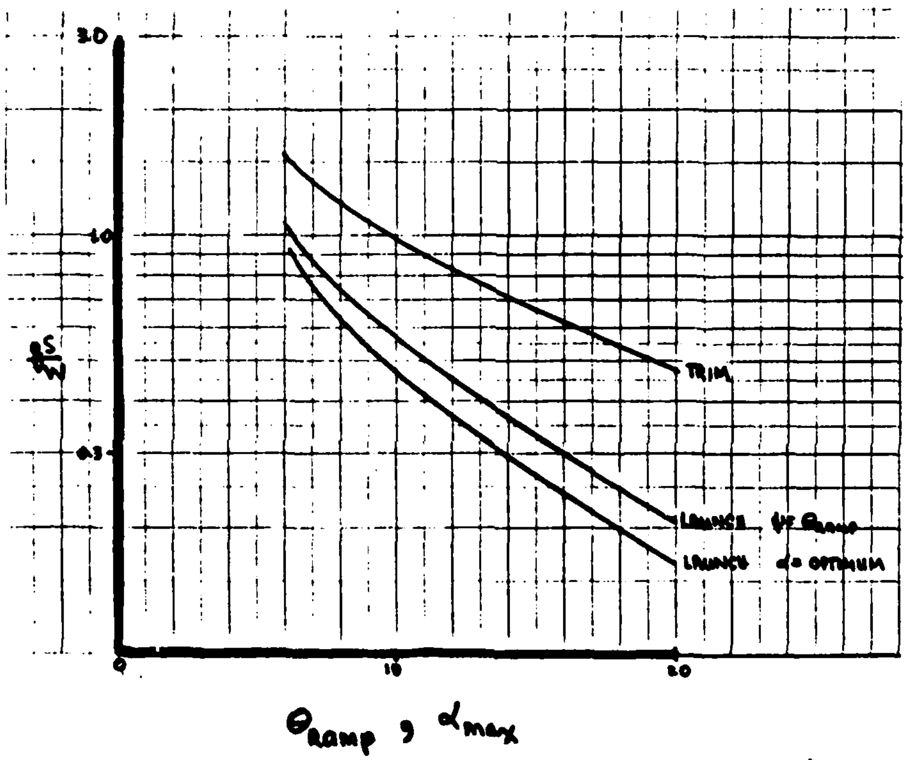

Figure 28. Launch and Trim Speeds for the F-15 for ψ = constant and $\alpha = \alpha_{optimum}$, T/W = 0.71

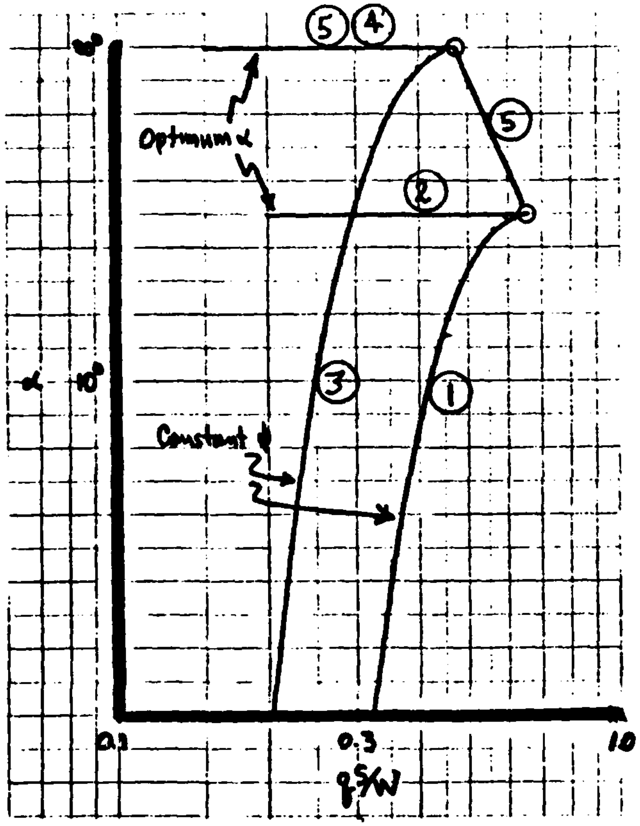

Figure 29. Angle of Attack

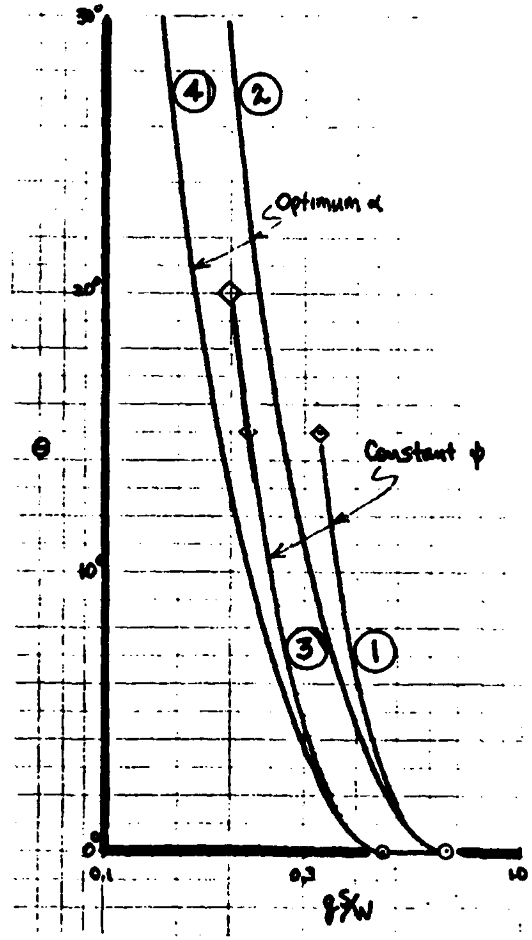

Figure 30. Climb Angle

Performance for $\alpha_{trim} \leq \alpha_{max}$

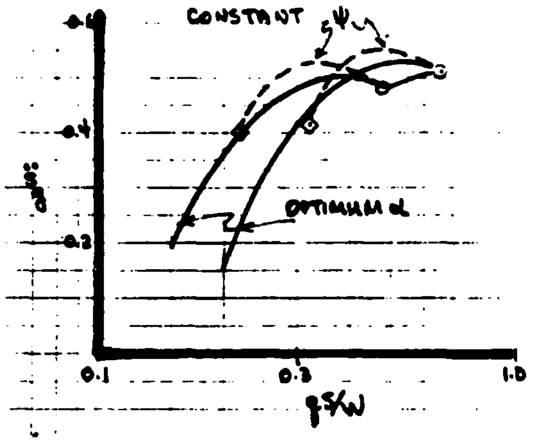

Figure 31. Acceleration Along the Flight Path

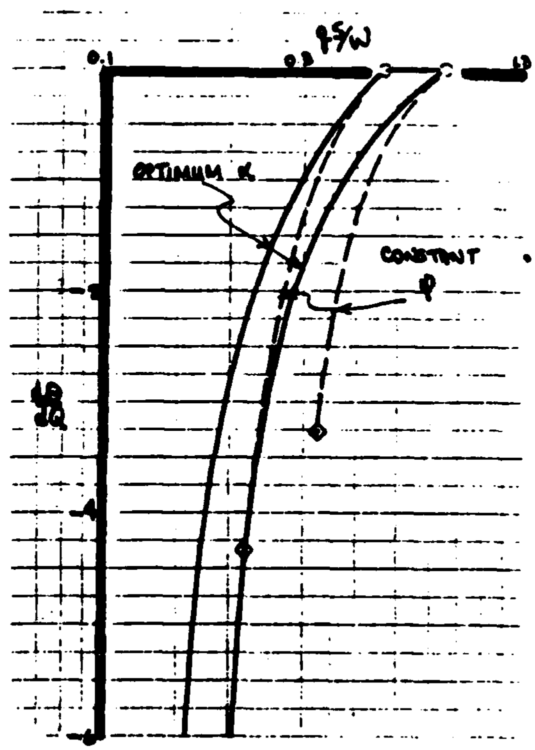

Figure 33. Efficiency

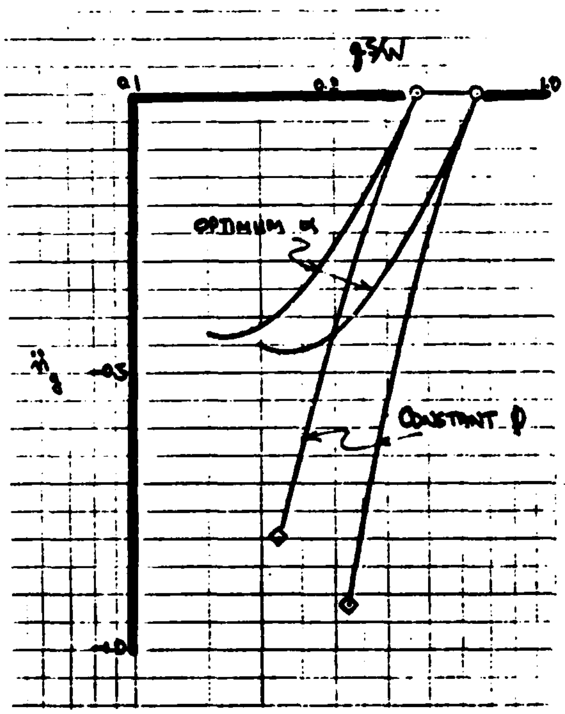

Figure 32. Acceleration Normal to the Flight Path

Performance for $\alpha_{trim} \leq \alpha_{max}$

END

FILMED

1-85

DTIC